ISSN (Print) 1226-1750
ISSN (Online) 2233-6656
Journal of Magnetics 30(4), 740-745 (2025) https://doi.org/10.4283/JMAG.2025.30.4.740

A Study on Metal Sputtering of 3D Printing Materials and Their Radiological Utility: Effects of Magnetic Materials on MRI Image Artifacts

Dayeong Hong and Hyeonggyun Kim*

Department of Radiological Science, Gimcheon University, Gimcheon, Gyeongsangbuk-do, 39528, Republic of Korea

(Received 28 October 2025, Received in final form 14 December 2025, Accepted 15 December 2025)

Conventional metal 3D printing has limitations in customized manufacturing and is expensive. Additionally, metal-printed objects can cause artifacts in radiological and MRI imaging when used in vivo. In contrast, polymer-based 3D printing is relatively cost-effective and accessible, resulting in its active application in the medical 3D printing field. Therefore, this study utilized FDM and SLA 3D printing technologies to produce specimens from various polymer materials and applied metal sputtering using titanium. The polymer-based metal-sputtered specimens were evaluated for their completeness using radiological imaging, and the compatibility and utility of the metal specimens were confirmed in MRI imaging. Through this research, a novel composite material and technique called polymer-based metal sputtering was proposed, which could serve as foundational research for the development of biocompatible composite materials in the future.

Keywords : 3D printing, metal sputtering, titanium, computed tomography, magnetic resonance imaging, metal artifact

1. Introduction

3D printing technology, based on additive manufacturing principles, has led to dramatic improvements in medical technology through various materials and techniques [1-3]. Traditional medical devices have struggled to incorporate diversity due to their reliance on mass production, leading to unmet demands for customized solutions. This is especially true for patients such as East Asians, children, the elderly, and individuals with disabilities [4, 5].

In this context, the medical field is increasingly utilizing advancements in 3D printing technology across various applications. Customized assistive devices, personalized bone structures for patients with bone loss, and tailored soft tissues for patients with skin ulcers are just a few examples of custom implants, surgical guides, and surgical tools being developed for individual needs [6-9]. Furthermore, recent developments in medical imaging, such as CT and MRI, allow for the identification of anatomical variations and diseases unique to each patient, enabling more accurate diagnoses and personalized treatment planning [10, 11]. In addition, the application of 3D printing technology in customized treatments facilitates precision medicine in diverse clinical settings [12].

However, there are still limitations in 3D printing technologies and materials that are suitable for clinical demand. Specifically, thermoplastic polymers, widely used as materials in medical 3D printing, offer various advantages such as their light weight, corrosion resistance, and cost-effectiveness, but they are significantly limited by their non-biocompatibility when directly inserted or applied in the human body. In response, recent advancements in metal 3D printing technologies utilizing metallic materials have begun to garner attention. SLS technology employs a laser to sinter powder materials, allowing the use of polymer, metal, and ceramic powders with high precision. However, this technology is accompanied by high output costs and complex post-processing challenges [13]. Direct metal laser sintering (DMLS) uses a laser to sinter metal powder materials, making it easier to produce high-strength products with complex geometries [14]. Nonetheless, high output costs, material expenses, and the prohibitive cost of printing equipment pose significant accessibility constraints [15].

Therefore, this study aims to combine biocompatible titanium metal sputtering with a variety of cost-effective and accessible polymer materials to verify radiological usability based on MRI compatibility.

*Corresponding author: Tel: +82-54-420-4177
Fax: +82-54-420-4003, e-mail: jung7818@hanmail.net

2. Materials and Methods

2.1. 3D Printing

The polymer materials for metal sputtering were designed using a 3D modeling program (Autodesk Fusion 360) to create cubic specimens measuring 20 mm × 20 mm × 20 mm. The specimens were printed using Fused Deposition Modeling (FDM) technology with thermoplastic polyurethane (TPU), acrylonitrile-butadiene-styrene (ABS), and polylactide (PLA). Additionally, specimens were printed using Stereolithography (SLA) technology with elastic, flexible, and clear resins (Formlabs Inc., Somerville, MA, USA), resulting in a total of six material specimens.

2.2. Metal Sputtering

Commonly used metal sputtering techniques include electrodeposition, electroless plating, spray technology, and physical vapor deposition (PVD). Among these, physical vapor deposition excels in its ability to deposit and maintain alloys compared to other thin-film techniques. It also has a high capability for depositing metals that are heat-resistant at high temperatures, making it suitable for forming thin films from metals or alloys with high melting points. As a result, it is widely used in various industries. Additionally, metal sputtering is relatively straightforward and provides uniform deposition, even on edges, facilitating surface treatment.

In this study, PVD magnetron sputtering was employed to perform a total of four depositions on the cubic specimens produced by 3D printing, and a titanium thin film was formed through plasma surface treatment (Fig. 1).

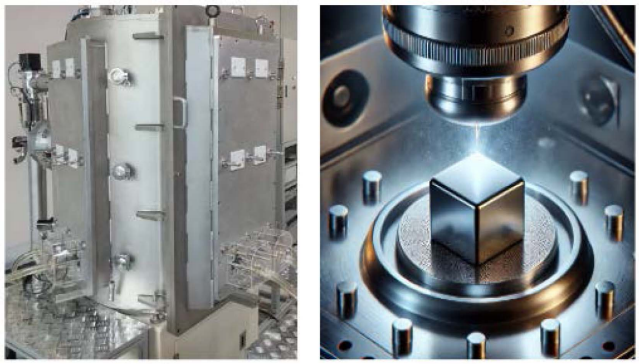

(A) (B)

Fig. 1. (Color online) Coating of 3D-printed specimens using the PVD magnetron sputtering technique. (A) PVD magnetron sputtering system, (B) Illustration of sputtering metal onto a 3D printed specimen.

2.3. Validation Experiment for Radiological Utility

Since this study aimed to account for various variables relevant to clinical practice, CT imaging was performed using equipment routinely used in hospital settings. CT imaging was conducted on six specimens to evaluate the shape and degree of metal sputtering in the samples (Revolution CT, GE Healthcare). Each specimen was secured with tape on a phantom filled with water. The CT scans were acquired with a cross-sectional thickness of 3.0 mm, and a visual assessment was performed using the Radiant DICOM viewer. The evaluation criteria included the measurability of the metal coating thickness, the infill status of the 3D-printed specimens, and the specimens'

(A) (B)

Fig. 2. (Color online) CT Imaging of 3D-printed specimens. (A) Metal-coated 3D-printed specimen fixed to the surface of the water phantom, (B) 3D-printed specimen undergoing CT imaging.

(A) (B)

Fig. 3. (Color online) MRI Imaging of 3D-printed specimens. (A) Metal-coated 3D-printed specimen fixed to the surface of the water phantom, (B) 3D-printed specimen undergoing MRI imaging.

surface morphology (Fig. 2).

2.4. Validation Experiment for Magnetic Resonance Imaging

To assess the extent of artifact generation in MRI images of each metal-sputtered specimen, two separate scans were conducted. Prior to imaging, each 3D-printed specimen was affixed to a water phantom using adhesive tape, with an alcohol swab placed on the superior cross-sectional surface of each specimen to aid in precise localization. An alcohol swab was placed on the specimen as an external marker to facilitate accurate localization and orientation during MRI acquisition. Two distinct MRI sequences were utilized in this study, including the

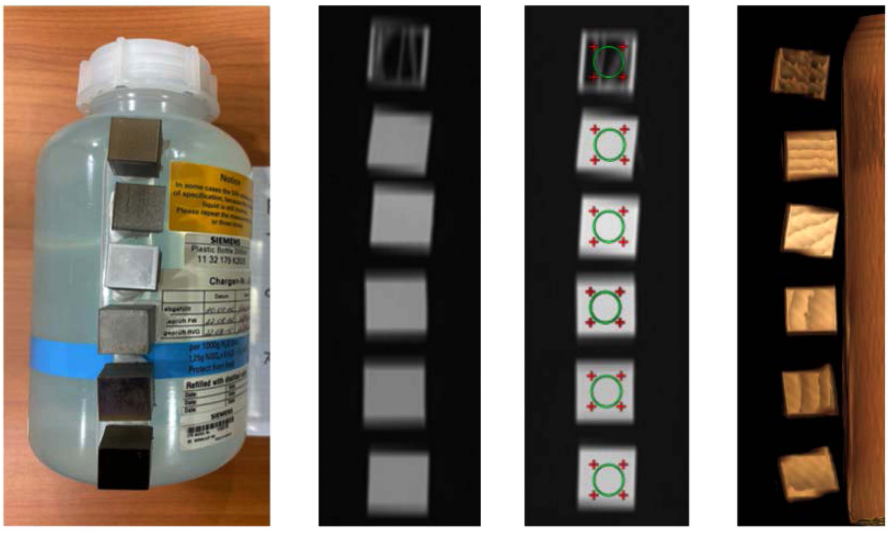

(A) (B) (C) (D)

Fig. 4. (Color online) CT images of 3D-printed specimens, from top to bottom: ABS, PLA, TPU, Clear resin, Elastic resin, Flexi resin. (A) Metal-coated 3D-printed specimen fixed to the surface of the water phantom, (B) CT image of the metal-coated 3D-printed specimen, (C) HU measurement of the CT image of the metal-coated 3D-printed specimen, (D) 3D volume rendering image of the metal-coated 3D-printed specimen.

Gradient Echo Imaging sequence, which is well-documented for its sensitivity to metal-induced artifacts, and the Spin Echo (SE) T1-weighted sequence. Following the acquisition of the imaging data, the artifacts associated with each material were visually assessed. The Signal-to-Noise Ratio (SNR) for each material was then quantitatively evaluated using 3D Slicer version 5.6.2, enabling a detailed comparison of image quality across the different materials (Fig. 3).

3. Results

3.1. Radiological Utility of 3D-Printed Samples

The cross-sectional thickness of the CT scans was found to be insufficient for measuring the coating thickness of the six metal sputtering specimens. However, slight differences in the cross-sectional shapes of the six specimens were observed in the CT images. Additionally, the internal filling rates of the six specimens were examined by measuring the Hounsfield units(HU). The SLA 3D-printed specimens all exhibited positive values, indicating relatively good internal filling. In contrast, among the FDM 3D-printed specimens, the ABS specimen showed negative values, suggesting insufficient internal filling (Fig. 4 and Table 1).

3.2. Compatibility of Magnetic Resonance Imaging for 3D-Printed Samples

The MRI images of samples with metal coatings exhibited distinct patterns depending on the imaging sequences employed. In particular, the Gradient Echo Imaging sequence, which is known to be highly sensitive to metal artifacts, demonstrated markedly greater visual differences when compared to the T1-weighted images, allowing for clear visual differentiation of the artifacts. Consequently, Signal-to-Noise Ratio (SNR) evaluation was conducted using a total of six samples that exhibited prominent artifacts in the Gradient Echo Imaging sequence (Figs. 5 and 6). The results revealed that the FDM material PLA exhibited the highest SNR, while the SLA material Flexi resin showed the lowest SNR values (Table 2). Despite the non-magnetic nature of FDM

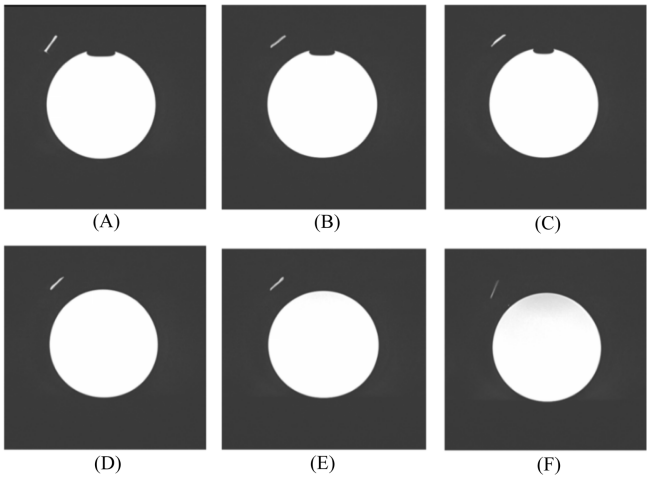

Fig. 5. Images of each specimen obtained using the Spin Echo (SE) T1 sequence. (A) ABS, (B) PLA, (C) TPU, (D) Clear resin, (E) Elastic resin, (F) Flexi resin.

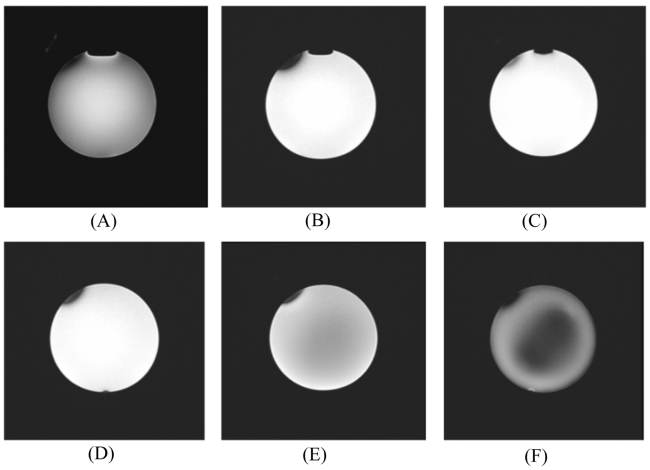

Fig. 6. Images of each specimen obtained using the Gradient Echo Imaging sequence. (A) ABS, (B) PLA, (C) TPU, (D) Clear resin, (E) Elastic resin, (F) Flexi resin.

Table 1. HU measurement of the CT image of the metal-coated 3D-printed specimen.

Material	ABS	PLA	TPU	Clear resin	Elastic resin	Flexi resin
HU	-815.14±129.97	100.46±5.42	180.88±5.38	100.80±3.81	14.73±3.59	48.4±3.89

Table 2. SNR measurement of the MRI image(Gradient Echo Imaging sequence) of the metal-coated 3D-printed specimen.

Material	ABS	PLA	TPU	Clear resin	Elastic resin	Flexi resin
Signal (mean±SD)	840.96±6.56	820.78±6.83	842.20±5.89	789.94±5.93	641.12±5.54	82.28±38.51
Noise (mean±SD)	57.13±34.88	46.18±17.62	342.32±35.45	121.58±19.80	188.26±29.16	221.35±6.97
SNR	24.11	46.58	24.44	39.88	21.99	5.75

materials such as ABS, PLA, and TPU, which typically have minimal impact on MRI imaging, the thin metal coatings applied to these materials still resulted in noticeable effects on the MRI images. In contrast, SLA resin materials, which can vary in magnetic properties depending on the type, and may contain metal components, demonstrated a broader range of imaging characteristics and SNR outcomes.

4. Discussion and Conclusion

This study was conducted using titanium, a material with high biocompatibility that is frequently used for medical implants. In particular, titanium is used as an artificial tooth root in dental implants due to its strong bonding properties with bone, allowing for stable fixation within the body. Additionally, it is lightweight, strong, and corrosion-resistant, making it suitable for bone screws, metal plates, and artificial joints in fracture treatments. Titanium also has advantages as a durable material for stents, which are used to expand blood vessels and maintain blood flow. However, titanium is a costly metal in terms of manufacturing and processing, making it less economically feasible. It is also harder and less elastic than bone, which can pose challenges for Osseo integration, and it may cause slight image distortions in MRI imaging. Therefore, this study aimed to provide foundational data for the use of polymer materials as implant materials by leveraging various hardness levels to reduce the elasticity mismatch with bone. Moreover, the lower metal content of the 3D-printed specimens could offer advantages in terms of MRI compatibility.

A significant finding of this study is that FDM materials exhibited relatively stable SNR values. This suggests that the inherently non-magnetic nature of acrylic materials is modified by the presence of a uniform external metal coating, which imparts magnetic properties. In contrast, SLA materials, composed of synthetic resins with diverse chemical characteristics, are more prone to alterations in MRI image quality due to their interaction with hydrogen. The observed differences in SNR and magnetic properties between FDM and SLA specimens may be attributed to variations in polymer composition and manufacturing processes. SLA materials undergo photopolymerization, which can result in denser structures and may influence titanium sputtering behavior. In contrast, FDM materials may exhibit different magnetic SNR characteristics due to their laminated structure and thermoplastic nature. Furthermore, some resin materials may incorporate metal components, emphasizing the necessity for a more comprehensive investigation of material properties in future research on MRI-integrated 3D printing.

However, this study has several limitations. PVD sputtering is a method that facilitates the formation of thin films from various metals. It is widely used in industry due to its stable process, high repeatability, and reproducibility. These features also resulted in its application in this study. However, the initial cost of equipment is extremely high, making it challenging to fully address the cost issues associated with metal 3D printing. Additionally, while image artifacts caused by titanium implants have been reported in clinical settings, previous studies indicate that titanium, as a non-ferrous metal, has very weak magnetic properties and does not significantly affect MRI imaging, raising potential questions about the validity of this study. Nevertheless, ongoing research into metal artifacts in MRI images suggests that titanium implants located near diseased areas can still cause localized artifacts.

In conclusion, this study presents a novel approach using 3D printing-based metal sputtering, which is a more accessible method. With further research, 3D printing-based titanium sputtering technology could contribute to the development and application of more advanced biocompatible composite materials.

Acknowledgments

This work was supported by the Gimcheon University Research Grant of 2024 (gc24005).

References

[1] Q. Yan, H. Dong, J. Su, J. Han, B. Song, Q. Wei, and Y. Shi, Engineering **4**, 729 (2018).
[2] A. Aimar, A. Palermo, and B. Innocenti, J. Healthc. Eng. **2019**, 5340616 (2019).
[3] W. Jamróz, J. Szafraniec, M. Kurek, and R. Jachowicz, Pharm. Res. **35**, 176 (2018).
[4] P. Tack, J. Victor, P. Gemmel, and L. Annemans, Biomed. Eng. Online **15**, 115 (2016).
[5] C. Y. Liaw and M. Guvendiren, Biofabrication **9**, 024102 (2017).
[6] T. Kim, S. Lee, G. B. Kim, D. Hong, J. Kwon, J. W. Park, and N. Kim, J. Prosthet. Dent. **124**, 195 (2020).
[7] B. Ma, T. Park, I. Chun, and K. Yun, J. Adv. Prosthodont. **10**, 279 (2018).
[8] E. Vorndran, C. Moseke, and U. Gbureck, MRS Bull. **40**, 127 (2015).
[9] A. A. Raheem, P. Hameed, R. Whenish, R. S. Elsen, A. K. Jaiswal, K. G. Prashanth, and G. Manivasagam, Biomimetics **6**, 65 (2021).
[10] V. Filippou and C. Tsoumpas, Med. Phys. **45**, e740

(2018).
[11] J. Parthasarathy, R. Krishnamurthy, A. Ostendorf, T. Shinoka, and R. Krishnamurthy, J. Magn. Reson. Imaging **51**, 1641 (2020).
[12] K. Park, H. Kim, and J. Cho, J. Magn. **22**, 508 (2017).
[13] R. Paudyal, H. Dong, T. R. Barrington, J. E. Warren, and E. Sala, Cancers **15**, 2573 (2023).
[14] C. Buchanan and L. Gardner, Eng. Struct. **180**, 332 (2019).
[15] W. K. Durfee and P. A. Iaizzo, Medical applications of 3D printing. In Engineering in Medicine, Academic Press, Oxford (2019) pp. 527-543.